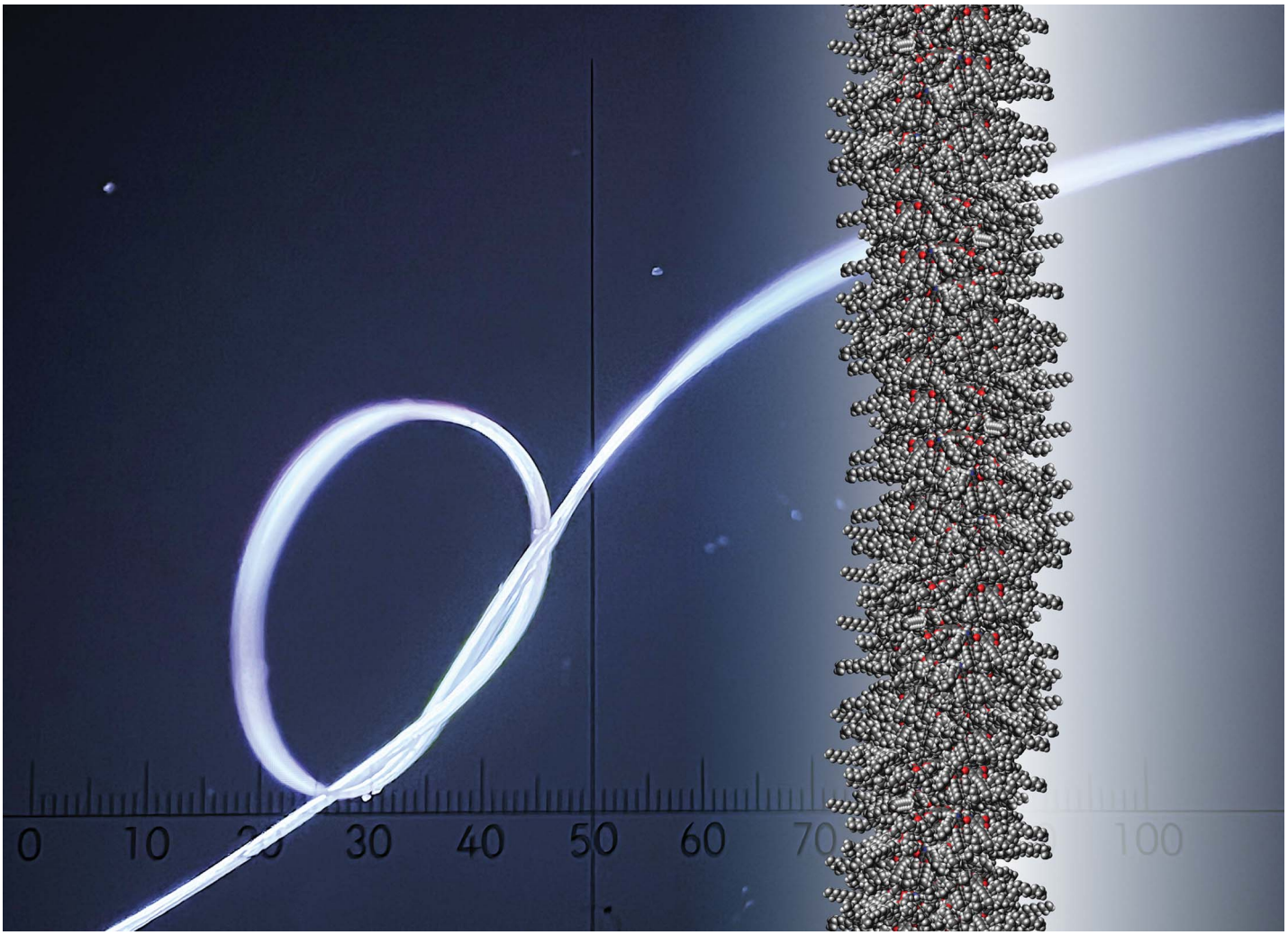

Showcasing research from Professor Sugiyasu's laboratory, Department of Polymer Chemistry, Kyoto University, Kyoto, Japan.

Individually separated supramolecular polymer chains toward solution-processable supramolecular polymeric materials

Random introduction of alkyl chains with different lengths onto a monomer prevented its supramolecular polymers from bundling, permitting the preparation of concentrated solutions of the supramolecular polymer without gelation, precipitation, or crystallization. With such a solution in hand, the authors succeeded in fabricating self-standing films and threads consisting of supramolecular polymers.

As featured in:

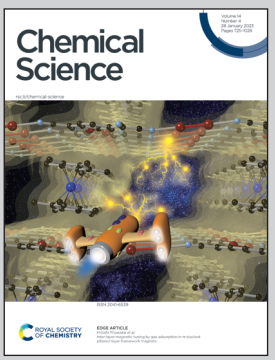

See Kazunori Sugiyasu *et al.*, *Chem. Sci.*, 2023, **14**, 822.

ROYAL SOCIETY OF CHEMISTRY

rsc.li/chemical-science

Registered charity number: 207890

Chemical Science

ROYAL SOCIETY OF CHEMISTRY

EDGE ARTICLE

View Article Online
View Journal | View Issue

Cite this: *Chem. Sci.*, 2023, **14**, 822

All publication charges for this article have been paid for by the Royal Society of Chemistry

Received 4th November 2022
Accepted 3rd January 2023

DOI: 10.1039/d2sc06089b

rsc.li/chemical-science

Individually separated supramolecular polymer chains toward solution-processable supramolecular polymeric materials†

Takuma Shimada, [ab] Yuichiro Watanabe, [c] Takashi Kajitani,[d] Masayuki Takeuchi, [b] Yutaka Wakayama [ab] and Kazunori Sugiyasu *[c]

Herein, we present a simple design concept for a monomer that affords individually separated supramolecular polymer chains. Random introduction of alkyl chains with different lengths onto a monomer prevented its supramolecular polymers from bundling, permitting the preparation of concentrated solutions of the supramolecular polymer without gelation, precipitation, or crystallization. With such a solution in hand, we succeeded in fabricating self-standing films and threads consisting of supramolecular polymers.

Introduction

Most supramolecular polymers can be categorized into two groups in terms of their polymerization mechanism: *i.e.*, isodesmic polymerization or nucleation–elongation polymerization.[1] In the latter mechanism, supramolecular polymerization is considered to occur in a similar manner to crystallization, except that it proceeds in one dimension exclusively. As such, seeded growth is possible (like crystallization), which has recently led to the development of living supramolecular polymerization and has opened a new door in supramolecular polymer chemistry.[2–6]

Although supramolecular polymerization is expected to proceed one-dimensionally in the above mechanism, in reality, this is not always the case. An increase in the monomer concentration leads to an increase in the degree of supramolecular polymerization, and at higher concentrations supramolecular polymers are prone to bundle, giving rise to gelation, precipitation, or crystallization. Consequently, solution processing of supramolecular polymers has been largely unexplored.[7–9] In this context, the purpose of the present study was to obtain individually separated supramolecular polymer chains at high concentrations (of the order of several mM).

Previously, Meijer and co-workers[10] have shown that deviations in the temperature-dependent spectra at high concentrations from those predicted by the nucleation–elongation model are caused by clustering (bundling) of supramolecular polymers. More recently, Giuseppone and co-workers[11] found that bundling of supramolecular polymers occurred either through coagulation or a secondary nucleation process, depending on the rate of cooling of the hot monomer solution. In common monomer designs for nucleated supramolecular polymerization, including the above two examples,[10,11] alkyl chains are introduced at the periphery of a monomer to endow the resultant supramolecular polymers with solubility by preventing three-dimensional crystallization. Nevertheless, bundling is practically inevitable. We hypothesized that engineering the surface of a supramolecular polymer chain by modifying the peripheral alkyl chains of its monomer might be effective in modulating lateral interactions between the supramolecular polymer chains.

Results and discussion

Supramolecular polymerization and bundling

In this study, we used triphenylene-based monomers[9,12] bearing six amide groups as intermonomer hydrogen-bonding sites. At the periphery of the triphenylene core, diverged through the amide linkages, eighteen octyl or octadecyl chains were introduced into monomers $\mathbf{1_8}$ and $\mathbf{1_{18}}$, respectively (Chart 1). Supramolecular polymerizations of monomers of this type are usually investigated in aliphatic solvents. We surmised that the solvation of the supramolecular polymers and, consequently, their bundling would be susceptible to subtle differences in the structure of the solvent molecule, so we screened linear [*e.g. n*-hexane (*n*Hex)], branched [isooctane (iOc)], and cyclic [*e.g.* cyclohexane (cHex)] aliphatic solvents [see the ESI; Fig. S8†].

[a]*Department of Chemistry and Biochemistry, Graduate School of Engineering, Kyushu University, Nishi-ku, Fukuoka 819-0395, Japan*

[b]*National Institute for Materials Science, Tsukuba, Ibaraki 305-0047, Japan*

[c]*Department of Polymer Chemistry, Kyoto University, Kyotodaigaku-katsura, Kyoto 615-8510, Japan. E-mail: sugiyasu.kazunori.8z@kyoto-u.ac.jp*

[d]*Open Facility Development Office, Open Facility Center, Tokyo Institute of Technology, 4259 Nagatsuta, Midori-ku, Yokohama 226-8503, Japan*

† Electronic supplementary information (ESI) available. See DOI: https://doi.org/10.1039/d2sc06089b

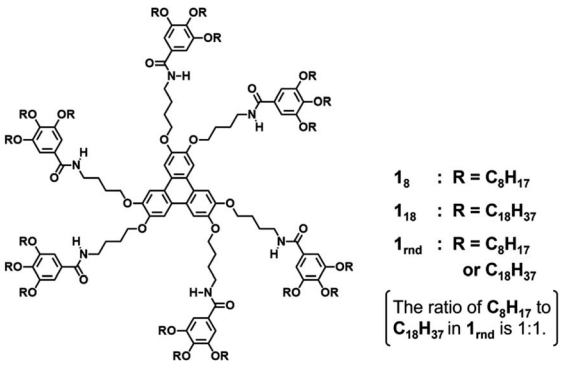

Chart 1 Structures of the monomers used in this study.

The $\mathbf{1_8}$ and $\mathbf{1_{18}}$ monomers were dissolved at a concentration of 50 μM in these solvents by heating, and the resultant solutions were left undisturbed at room temperature. Both monomers readily underwent one-dimensional (1D) supramolecular polymerization in *n*Hex or iOc, and heavily bundled fibrous aggregates were observed by atomic force microscopy (AFM) (Fig. 1). In cHex, supramolecular polymerization of $\mathbf{1_8}$ occurred relatively slowly (see below), and $\mathbf{1_{18}}$ did not form a 1D supramolecular polymer within our experimental timescale (several months: see ESI,† Fig. S9). These results suggest that differences in the nature of the solvent molecule affect the supramolecular polymerization kinetics but do not significantly affect the lateral interaction between supramolecular polymer chains. In addition, the length of the alkyl chains (C_8H_{17} *vs.* $C_{18}H_{37}$) in a monomer appears not to be a critical factor from a viewpoint of the purpose of this study.

To gain an insight into the bundling process, we attempted to capture the evolution of bundles of supramolecular polymers of $\mathbf{1_8}$. This was possible in cHex, owing to the slow rate of supramolecular polymerization in this solvent. After cooling the hot monomer solution, aliquots of the solution were spin-coated onto a highly oriented pyrolytic graphite (HOPG) substrate at various times for AFM measurements. Even in the earliest stages (30 minutes after cooling), short supramolecular polymers had assembled laterally, indicating the occurrence of secondary nucleation (Fig. 2a).[13] Over time, fibrous aggregates grew further through elongation and bundling (Fig. 2b and c). Finally, precipitates displaying birefringence appeared (Fig. S10†), thus suggesting that agglomeration observed throughout the above processes occurred in solution and not on the HOPG substrate. This result clearly indicates that the triphenylene-based supramolecular polymers have a strong propensity to undergo bundling.

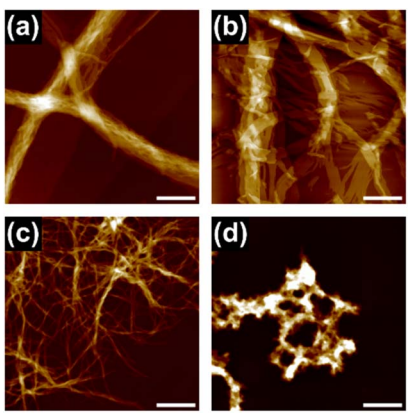

Fig. 1 AFM images of supramolecular polymers of (a and b) $\mathbf{1_8}$ and (c and d) $\mathbf{1_{18}}$ prepared in (a and c) *n*Hex and (b and d) iOc: 50 μM; highly oriented pyrolytic graphite (HOPG) substrates; scale bar = (a and b) 200 nm and (c and d) = 1 μm.

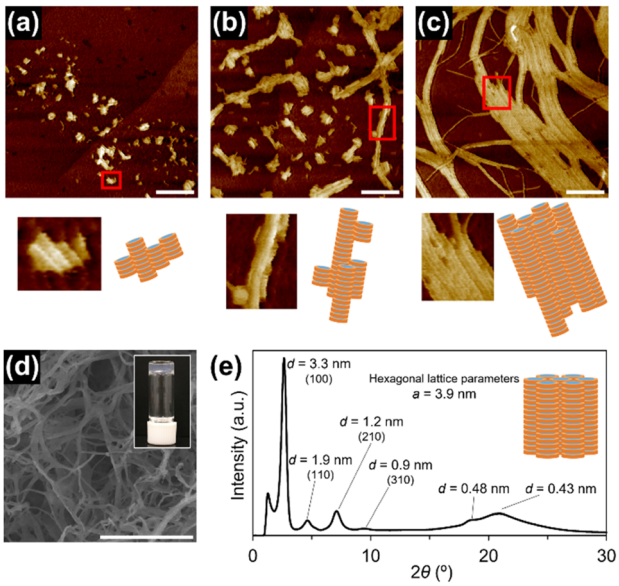

Fig. 2 Successive AFM images of supramolecular polymers captured at (a) 30 min, (b) 60 min, and (c) 90 min after cooling a hot 50 μM solution of $\mathbf{1_8}$ in cHex; scale bar = 100 nm. The solution was stirred at 400 rpm at room temperature. (d) SEM image (scale bar = 5 μm) of the xerogel of $\mathbf{1_8}$ prepared from a 1 mM solution in cHex, (inset) photograph of the organogel. (e) XRD pattern of the xerogel of $\mathbf{1_8}$.

At a higher concentration (1 mM), $\mathbf{1_8}$ formed a translucent or opaque gel, suggesting the formation of large aggregates capable of scattering visible light (ESI; Fig, S8a†), whereas $\mathbf{1_{18}}$ precipitated in most of the solvents tested (ESI; Fig. S8b†). A xerogel of $\mathbf{1_8}$ freeze-dried from cHex consisted of a dense network of thick fibrous aggregates with diameters of 50 nm−1.5 μm, as observed by scanning electron microscopy (SEM) (Fig. 2d). Powder X-ray diffraction (XRD) measurement of the xerogel showed clear diffraction peaks attributable to a hexagonal packing of 1D columns of $\mathbf{1_8}$ (Fig. 2e). Because of the crystalline nature of the aggregates, the organogels readily collapsed upon mechanical agitation, and solid materials separated out in the solvent (ESI; Fig. S11†), which made it difficult to process the supramolecular polymers to form films or threads. These results confirmed that lateral interactions between 1D supramolecular polymer chains dictates macroscopic properties of supramolecular polymers.

A new monomer design: random introduction of peripheral alkyl chains

Although octyl and octadecyl chains were individually found to be unsuitable for the purposes of this study, we surmised that

a random mixture of the two types of chain might lead to a different situation. With this in mind, we designed a new monomer $\mathbf{1_{rnd}}$ in which octyl and octadecyl chains were randomly introduced ($\mathbf{1_{rnd}}$ in Chart 1). We expected that the randomness of the side chains would perturb the surfaces of the supramolecular polymer chains and would prevent them from bundling (Fig. 3c). To this end, the ratio of the two types of alkyl chain in a monomer is a matter of interest, and our first choice was 1 : 1 molar ratio, as it had been reported in a study on self-assembled monolayers (SAMs) that the greatest degree of disorder in a longer alkanethiolate was observed with equimolar amounts of a shorter alkanethiolate.[14] In $\mathbf{1_{rnd}}$, statistically there are about 8000 possible combinations (*i.e.*, distinct monomers) in terms of the proportions and positions of the two alkyl chains. The average number of the octadecyl chains in a monomer is nine; monomers with nine such units comprise 18.5% of the mixture (Fig. 4c). Monomers with fewer than six or more than twelve octadecyl chains are in the minority (4.8% each), and the proportion substituted exclusively with octyl or octadecyl chain (*i.e.*, $\mathbf{1_8}$ and $\mathbf{1_{18}}$) is negligible (0.0004%). The synthesis of $\mathbf{1_{rnd}}$ was straightforward (Fig. 4a, see ESI; Scheme S1 and S2†). First, 1 : 1 mixture of 1-bromooctane and 1-bromooctadecane was reacted with methyl 3,4,5-trihydroxybenzoate (methyl gallate) to afford $\mathbf{2_{rnd}}$. Using the mixture of precursors bearing octyl or octadecyl chains (Fig. 4b), $\mathbf{1_{rnd}}$ was synthesised through common reactions. The number of aliphatic protons in $\mathbf{1_{rnd}}$ determined by ^{1}H NMR spectroscopy agreed with the expected average value (ESI; Fig. S2†). MALDI-TOF mass spectrometry showed the presence of monomers with distinct molecular weights (ESI; Fig. S12†). These results

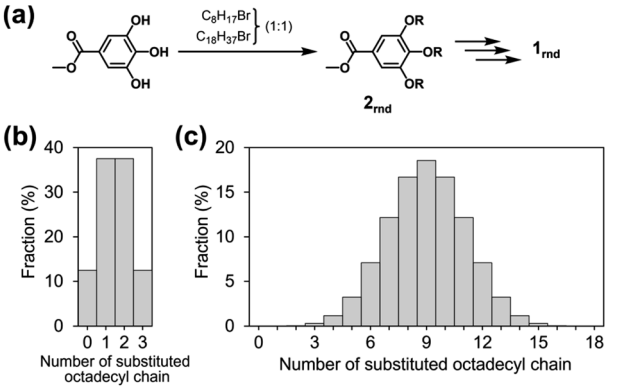

Fig. 4 (a) Random introduction of two different alkyl chains and synthesis of $\mathbf{1_{rnd}}$. The proportions of the octadecyl chains in (b) precursor $\mathbf{2_{rnd}}$ and (c) monomer $\mathbf{1_{rnd}}$.

confirmed the random introduction of octyl and octadecyl chains to the triphenylene core.

Supramolecular polymerization of $\mathbf{1_{rnd}}$ was investigated in a variety of aliphatic solvents. At a relatively high concentration (1 mM), $\mathbf{1_{rnd}}$ formed transparent organogels in linear or branched aliphatic solvents. In contrast to organogels of $\mathbf{1_8}$ (see above), those of $\mathbf{1_{rnd}}$ were converted into homogeneous solutions upon mechanical agitation (ESI; Fig. S13†). In addition, after 2 days, the organogel reformed without any precipitation or phase separation (so-called thixotropic behaviour). AFM measurements showed that bundling was suppressed with $\mathbf{1_{rnd}}$ (50 μM in *n*Hex and iOc; Fig. 3a and b). For comparison, we investigated the supramolecular copolymerization of $\mathbf{1_8}$ and $\mathbf{1_{18}}$

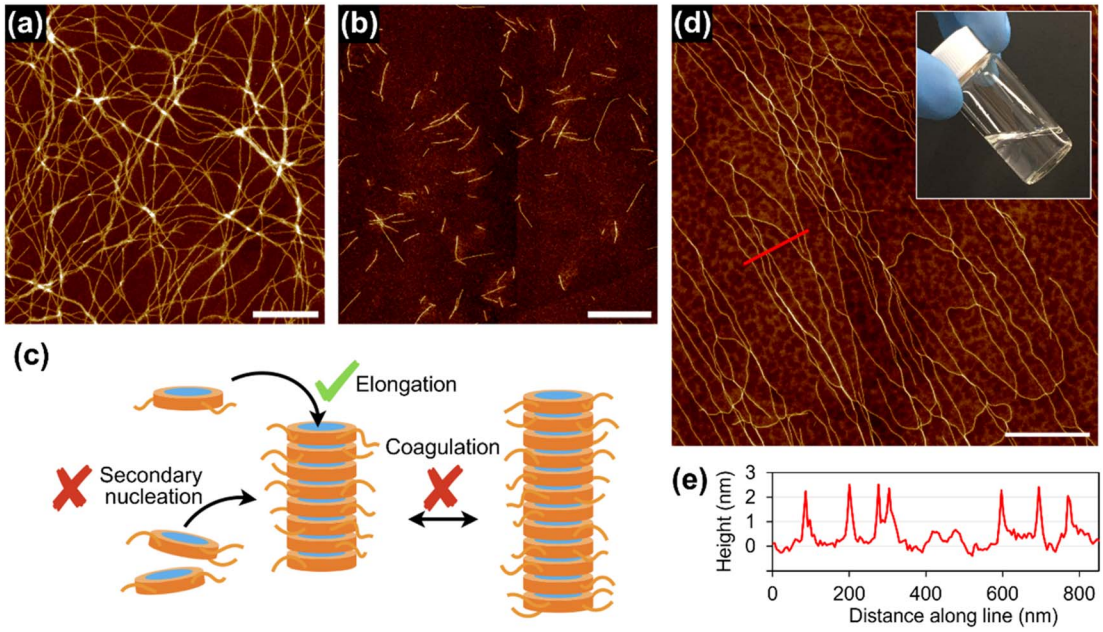

Fig. 3 AFM images of supramolecular polymers of $\mathbf{1_{rnd}}$ prepared in (a) *n*Hex and (b) iOc (50 μM); scale bar = 300 nm. (c) Schematic representation of supramolecular polymerization of $\mathbf{1_{rnd}}$; bundling processes appear to be prevented owing to the surface engineering. (d) AFM image of individually separated supramolecular polymer chains of $\mathbf{1_{rnd}}$ prepared by seeded supramolecular polymerization in a cHex/iOc mixed solvent (1 mM); scale bar = 1 μm. (inset) photograph of the solution containing it. (e) Height measurements across the green line on (d).

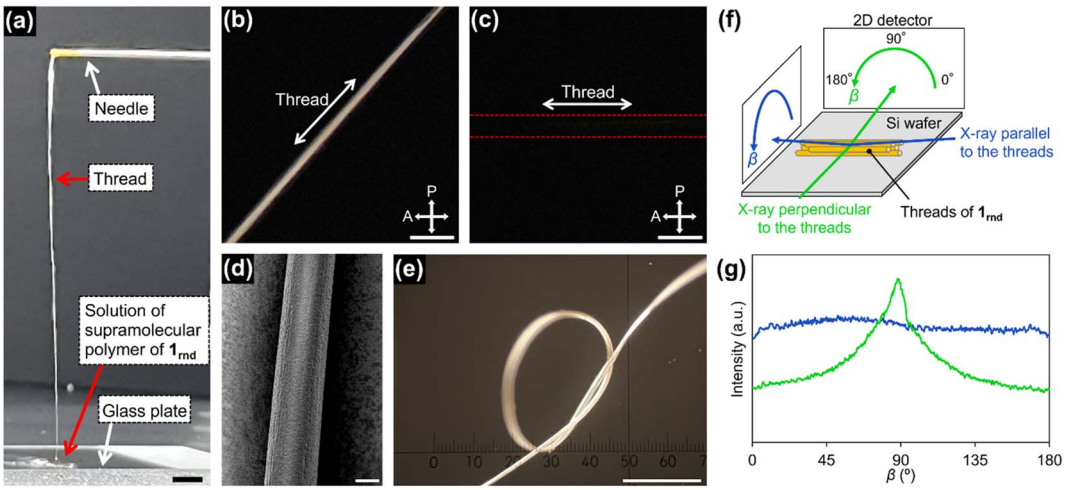

Fig. 5 (a) Photograph of a thread drawn from a concentrated solution of $\mathbf{1_{rnd}}$ prepared by seeded polymerization (Fig. 3d): scale bar = 5 mm. POM images of the thread on a glass substrate with the thread rotated (b) 45°and (c) 0°/90°with respect to the polarizer/analyser: scale bar = 100 μm. (d) SEM image of the thread: scale bar = 20 μm. (e) Optical micrograph of a knotted thread: scale bar = 500 μm. (f) Schematic representation of the experimental setup for 2D GI-WAXD. (g) Angle-dependence of the peak intensity for $2\theta = 1.7°–2.7°$ (*ca.* 3.9 nm) in the 2D GI-WAXD with respect to β, as shown in (f).

(1 : 1 molar ratio [$\mathbf{1_8}$ + $\mathbf{1_{18}}$] = 1 mM in *n*Hex); the resulting organogel consisted of bundled supramolecular polymer chains and did not show the abovementioned thixotropic behaviour (ESI; Fig. S14†). We infer that $\mathbf{1_8}$ and $\mathbf{1_{18}}$ do not copolymerize completely randomly because of the difference in their supramolecular polymerization kinetics.

As in the case of $\mathbf{1_{18}}$, $\mathbf{1_{rnd}}$ did not undergo spontaneous supramolecular polymerization in cHex. However, the addition of short supramolecular polymers of $\mathbf{1_{rnd}}$ prepared in iOc (Fig. 3b) as 'seeds' to the cHex solution of $\mathbf{1_{rnd}}$ initiated its 1D supramolecular polymerization (ESI; Fig. S15†). For reference, $\mathbf{1_{18}}$ was unable to form 1D supramolecular polymers with the addition of the seeds of $\mathbf{1_{rnd}}$. Interestingly, the seeded supramolecular polymerization did not result in the formation of an organogel, but instead afforded a viscous solution, even at a higher concentration (1 mM). We infer that the supramolecular polymers propagated in a controlled fashion in terms of their primary and secondary nucleation processes through the seeded growth. Gratifyingly, very long, individually separated supramolecular polymer chains were observed in the viscous solution (Fig. 3d and e and S16; ESI†).

Solution processing of supramolecular polymer

With this concentrated solution of the supramolecular polymer in hand, we were able to fabricate self-standing films (ESI; Fig. S17†) and threads. For example, a thread about 10 cm long was manually drawn from the solution by using a needle (Fig. 5a). Polarized optical microscopy (POM) under crossed polarizers revealed that supramolecular polymers of $\mathbf{1_{rnd}}$ were highly aligned along the thread (Fig. 5b and c). We carried out grazing-incident wide-angle X-ray diffraction (GI-WAXD) measurements with the X-ray beam parallel and perpendicular to the long axis of the threads (Fig. 5f). Although weak in intensity, a diffraction with a *d* spacing of 3.9 nm, consistent with the diameter of $\mathbf{1_{rnd}}$, was observed by two-dimensional (2D) WAXD. The diffraction was observed as an anisotropic and an isotropic pattern with respect to the angle β (Fig. 5f) when the incident X-ray beam were perpendicular and parallel to the long axis of the thread, respectively. This result indicates that supramolecular polymers were aligned along the long axis of the thread (Fig. 5g). Remarkably, the dried thread was sufficiently flexible to permit it to be tied in a knot (Fig. 5e). It should be noted that such homogeneous solution processing was not possible with individual $\mathbf{1_8}$, $\mathbf{1_{18}}$, or the mixture of $\mathbf{1_8}$ and $\mathbf{1_{18}}$ (ESI; Fig. S14†). This result demonstrated an advantage of introducing randomness at the monomer level.

Conclusions

In conclusion, we presented a simple molecular-design concept to obtain individually separated supramolecular polymer chains in organic solvents. It has previously been shown that electrostatic repulsion is effective in preventing bundling of supramolecular polymer chains; however, this type of strategy is generally limited to supramolecular polymerization in aqueous media.[7] By using the randomized monomer $\mathbf{1_{rnd}}$, we demonstrated that engineering the surface of supramolecular polymer chains is effective in disturbing lateral interactions, such as chain–chain coagulation and surface-catalyzed secondary nucleation. As a result, concentrated solutions of individually separated supramolecular polymer chains could be prepared that permitted solution processing of the supramolecular polymer. We believe that control over the lateral interaction among supramolecular polymer chains is of great importance not only for creation of higher-order mesoscopic structures[5,15] but also for materialization of supramolecular polymers.[16] Rheological studies on concentrated solutions, films, and threads containing the resulting supramolecular polymers are in progress.

Data availability

The data supporting this study are provided in the ESI.†

Author contributions

K. S. conceived the project. T. S. synthesized the monomers, characterized their supramolecular polymerization, and prepared supramolecular polymeric materials. T. K. conducted XRD measurements. All authors discussed the results. T. S. and K. S. wrote the paper with input from all the authors.

Conflicts of interest

There are no conflicts to declare.

Acknowledgements

We are grateful to Prof. Kazuo Tanaka (Kyoto University) for use of a polarized optical microscope. The authors thank Prof. Hiroshi Endo (Toyama Prefectural University) for a fruitful discussion. This work was supported by Grants-in-Aid Scientific Research (22H02134), a Grant-in Aid for Scientific Research on Innovative Arias "Soft Crystals" (20H04682), and a Grant-in-Aid for Transformative Research Areas (A) "Condensed Conjugation" (JP20H05868), and Data Creation and Utilization-Type Material Research and Development Project (JPMXP1122714694). Financial support from The Izumi Science and Technology Foundation, The Iketani Science and Technology Foundation, The Murata Science Foundation, Sekisui Chemical Grant Program, and The Mitsubishi Foundation are also acknowledged. T.S. thanks the Japan Society for the Promotion of Science for a research fellowship for young scientist (22J11922).

Notes and references

1 (*a*) D. Zhao and J. S. Moore, *Org. Biomol. Chem.*, 2003, **1**, 3471–3491; (*b*) T. F. A. De Greef, M. M. J. Smulders, M. Wolffs, A. P. H. J. Schenning, R. P. Sijbesma and E. W. Meijer, *Chem. Rev.*, 2009, **109**, 5687–5754; (*c*) M. Hartlieb, E. D. H. Mansfield and S. Perrier, *Polym. Chem.*, 2020, **11**, 1083–1110.

2 M. Wehner and F. Würthner, *Nat. Rev. Chem.*, 2020, **4**, 38–53.

3 (*a*) S. Ogi, K. Sugiyasu, S. Manna, S. Samitsu and M. Takeuchi, *Nat. Chem.*, 2014, **6**, 188–195; (*b*) J. Kang, D. Miyajima, T. Mori, Y. Inoue, Y. Itoh and T. Aida, *Science*, 2015, **347**, 646–651; (*c*) S. Ogi, V. Stepanenko, K. Sugiyasu, M. Takeuchi and F. Würthner, *J. Am. Chem. Soc.*, 2015, **137**, 3300–3307; (*d*) M. Endo, T. Fukui, S. H. Jung, S. Yagai, M. Takeuchi and K. Sugiyasu, *J. Am. Chem. Soc.*, 2016, **138**, 14347–14353; (*e*) M. E. Robinson, A. Nazemi, D. J. Lunn, D. W. Hayward, C. E. Boott, M. Hsiao, R. L. Harniman, S. A. Davis, G. R. Whittell, R. M. Richardson, L. De Cola and I. Manners, *ACS Nano*, 2017, **11**, 9162–9175; (*f*) J. S. Valera, R. Gómez and L. Sánchez, *Small*, 2018, **14**, 1702437; (*g*) T. Fukui, N. Sasaki, M. Takeuchi and K. Sugiyasu, *Chem. Sci.*, 2019, **10**, 6770–6776.

4 T. Fukui, S. Kawai, S. Fujinuma, Y. Matsushita, T. Yasuda, T. Sakurai, S. Seki, M. Takeuchi and K. Sugiyasu, *Nat. Chem.*, 2017, **9**, 493–499.

5 N. Sasaki, M. F. J. Mabesoone, J. Kikkawa, T. Fukui, N. Shioya, T. Shimoaka, T. Hasegawa, H. Takagi, R. Haruki, N. Shimizu, S. Adachi, E. W. Meijer, M. Takeuchi and K. Sugiyasu, *Nat. Commun.*, 2020, **11**, 3578.

6 (*a*) S. H. Jung, D. Bochicchio, G. M. Pavan, M. Takeuchi and K. Sugiyasu, *J. Am. Chem. Soc.*, 2018, **140**, 10570–10577; (*b*) W. Wagner, M. Wehner, V. Stepanenko and F. Würthner, *J. Am. Chem. Soc.*, 2019, **141**, 12044–12054; (*c*) A. Sarkar, R. Sasmal, A. Das, S. S. Agasti and S. J. George, *Chem. Commun.*, 2021, **57**, 3937–3940.

7 (*a*) S. Zhang, M. A. Greenfield, A. Mata, L. C. Palmer, R. Bitton, J. R. Mantei, C. Aparicio, M. O. De La Cruz and S. I. Stupp, *Nat. Mater.*, 2010, **9**, 594–601; (*b*) T. Christoff-Tempesta, Y. Cho, D. Kim, M. Geri, G. Lamour, A. J. Lew, X. Zuo, W. R. Lindemann and J. H. Ortony, *Nat. Nanotechnol.*, 2021, **16**, 447–454.

8 M. Hecht, B. Soberats, J. Zhu, V. Stepanenko, S. Agarwal, A. Greiner and F. Würthner, *Nanoscale Horiz.*, 2019, **4**, 169–174.

9 H. Zhang, J. Cheng, Q. Zhou, Q. Zhang and G. Zou, *Soft Matter*, 2020, **16**, 5203–5209.

10 P. Jonkheijm, P. van der Schoot, A. P. H. J. Schenning and E. W. Meijer, *Science*, 2006, **313**, 80–83.

11 A. Osypenko, E. Moulin, O. Gavat, G. Fuks, M. Maaloum, M. A. J. Koenis, W. J. Buma and N. Giuseppone, *Chem. – Eur. J.*, 2019, **25**, 13008–13016.

12 (*a*) M. Ikeda, M. Takeuchi and S. Shinkai, *Chem. Commun.*, 2003, 1354–1355; (*b*) Y. Tatewaki, T. Hatanaka, M. Kimura and H. Shirai, *Chem. Lett.*, 2009, **38**, 900–901; (*c*) Y. Li, Y. Wang, X. Ren and L. Chen, *Mater. Chem. Front.*, 2017, **1**, 2599–2605; (*d*) M. L. Ślęczkowski, M. F. J. Mabesoone, P. Ślęczkowski, A. R. A. Palmans and E. W. Meijer, *Nat. Chem.*, 2021, **13**, 200–207; (*e*) M. L. Ślęczkowski, M. F. J. Mabesoone, M. D. Preuss, Y. Post, A. R. A. Palmans and E. W. Meijer, *J. Polym. Sci.*, 2022, **60**, 1871–1877.

13 M. Törnquist, T. C. T. Michaels, K. Sanagavarapu, X. Yang, G. Meisl, S. I. A. Cohen, T. P. J. Knowles and S. Linse, *Chem. Commun.*, 2018, **54**, 8667–8684.

14 P. E. Laibinis, R. G. Nuzzo and G. M. Whitesides, *J. Phys. Chem.*, 1992, **96**, 5097–5105.

15 S. Datta, Y. Kato, S. Higashiharaguchi, K. Aratsu, A. Isobe, T. Saito, D. D. Prabhu, Y. Kitamoto, M. J. Hollamby, A. J. Smith, R. Dalgliesh, N. Mahmoudi, L. Pesce, C. Perego, G. M. Pavan and S. Yagai, *Nature*, 2020, **583**, 400–405.

16 R. Laishram, S. Sarkar, I. Seth, N. Khatun, V. K. Aswal, U. Maitra and S. J. George, *J. Am. Chem. Soc.*, 2022, **144**, 11306–11315.